THE FINITE LAYER METHOD FOR GROUNDWATER FLOW MODELS

Stanley S. Smith
Jay Puckett
Myron B. Allen
Thomas Edgar

1992
Journal Article
WWRC-92-13

In

Water Resources Research

Volume 28, Number 6

Submitted by

Stanley S. Smith
Myron B. Allen
Department of Mathematics

and

Jay Puckett
Thomas Edgar
Department of Civil Engineering

University of Wyoming
Laramie, Wyoming

WATER RESOURCES RESEARCH, VOL. 28, NO. 6, PAGES 1715–1722, JUNE 1992

The Finite Layer Method for Groundwater Flow Models

STANLEY S. SMITH AND MYRON B. ALLEN

Department of Mathematics, University of Wyoming, Laramie

JAY PUCKETT AND THOMAS EDGAR

Department of Civil Engineering, University of Wyoming, Laramie

The finite layer method (FLM) is an extension of the finite strip method familiar in structural engineering. The idea behind the method is to discretize two space dimensions using truncated Fourier series, approximating variations in the third via finite elements. The eigenfunctions used in the Fourier expansions are orthogonal, and, consequently, the Galerkin integrations decouple the weighted residual equations associated with different Fourier modes. The method therefore reduces three-dimensional problems to sets of independent matrix equations that one can solve either sequentially on a microcomputer or concurrently on a parallel processor. The latter capability makes the method suitable for such computationally intensive applications as optimization and inverse problems. Four groundwater flow applications are presented to demonstrate the effectiveness of FLM as a forward solver.

1. INTRODUCTION

The finite layer method (FLM) is a numerical method that shows promise for modeling many aquifer flow problems. The idea behind the method is to discretize one dimension of the spatial domain using finite elements, approximating variations in the other two dimensions using truncated Fourier series. For problems having sufficient geometric simplicity this approach avoids much of the expense associated with three-dimensional finite elements. When the Fourier series is composed of orthogonal eigenfunctions, the finite element integration decouples the equation sets for different Fourier modes, and it is therefore possible to solve many small, simultaneous matrix equations in parallel. This inherent parallelism can be especially important when it is necessary to execute a flow model iteratively, as in parameter identification and optimization studies. This paper examines the application of the FLM to several problems of interest to groundwater hydrologists.

Much of the literature relevant to the FLM concerns its predecessor, the finite strip method (FSM) [*Cheung*, 1976], and applications to structural engineering. The FSM uses truncated Fourier series to discretize problems along one coordinate axis instead of two. *Puckett and Wiseman* [1987] review the literature on the FSM pertaining to structural analysis. The FLM itself has received some attention, for example, in the analysis of elastic, horizontally layered foundations [*Cheung and Fan*, 1979]. It is also possible to extend the FLM to problems with infinite layers having finite thickness. *Rowe and Booker* [1982] apply this technique to elastic soils, as do *Small and Booker* [1984*a*]. *Booker and Small* [1982*a*, *b*, 1986] also use this approach to model soil consolidation and surface deformation accompanying the extraction of water [*Small and Booker*, 1984*b*]. *Slattery* [1986] and, subsequently, *Puckett and Schmidt* [1990] utilize the FSM to obtain head distributions in two-dimensional well drawdown models.

Paper number 92WR00425.
0043-1397/92/92WR-00425$05.00

One way to think of the FLM is as a quasi-analytic method, in which one incorporates analytic information about the initial boundary value problem (in this case, the eigenfunctions of the spatial operator) into the numerical approximation. Other quasi-analytic methods, similar in spirit but different in detail, have appeared in the water resources literature, including the finite analytic method [*Hwang et al.*, 1985] and the Laplace transform Galerkin method [*Sudicky*, 1989], among others. The FLM is also related to the spectral method [*Gottlieb and Orszag*, 1977]. The two methods share the idea of approximating spatial variations using truncated series of eigenfunctions. Where they differ is in the use of finite element approximations to discretize problems along one of the three spatial coordinates in the FLM. This device facilitates the simulation of certain geometrically simple heterogeneities, such as those occurring in stratified sedimentary basins.

In this paper we present the formulation of the FLM, discuss several coding aspects of the method, and demonstrate its application to four problems. The first problem involves a fully penetrating well; the second involves injection of water at a single point in the aquifer; the third is a three-dimensional model of a leaky aquifer; and the fourth is a model of a multiwell field. We do not present a full error analysis for the method, which is logically the subject of another article. Such an analysis would clarify the trade-offs between accuracy and computational effort, both in the choice of Fourier discretizations and in the finite element gridding.

2. FORMULATION OF THE FINITE LAYER METHOD

The FLM rests on certain geometric assumptions about the problem's spatial domain $\mathcal{D}$. In particular, we consider $\mathcal{D}$ to be a rectangular parallelepiped consisting of a saturated, confined aquifer in which Darcy's law applies. We assume that the coordinate axes coincide with the principal directions of the hydraulic conductivity tensor and that principal hydraulic conductivities K_x, K_y, and K_z vary only with elevation z above datum. These assumptions are reasonable

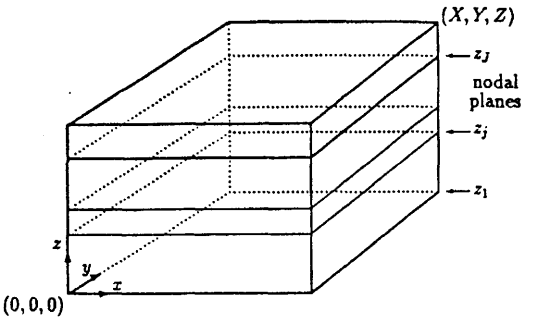

Fig. 1. Typical rectangular parallelepiped domain $\mathcal{D}$.

in many sedimentary formations where the bedding planes are nearly parallel. Figure 1 depicts a typical domain $\mathcal{D}$ with dimensions X, Y, and Z.

We begin by establishing the boundary value problem to be solved and define the differential operator $L[\ ]$ as follows:

$$L[h] = -K_x \frac{\partial^2 h}{\partial x^2} - K_y \frac{\partial^2 h}{\partial y^2} - \frac{\partial}{\partial z}\left(K_z \frac{\partial h}{\partial z}\right) + S_s \frac{\partial h}{\partial t}. \tag{1}$$

Here S_s is the specific storage. Under our assumptions the equation governing the head $h(x, y, z, t)$ is

$$L[h] + F = 0, \tag{2}$$

where the prescribed forcing function $F(x, y, z, t)$ gives the rate of water withdrawal per unit volume of porous medium. We refer readers to *Huyakorn and Pinder* [1983] and *Walton* [1970] for the derivation of (2).

When the withdrawal (or injection) occurs at a point sink or source, one can take F to be a possibly time-dependent multiple of the Dirac δ distribution. Superpositions of such distributions, centered at different spatial points, are also possible, as are more general functional forms. As with most discrete methods, the FLM has a limited ability to capture the steep head gradients that occur near point sources and sinks. In the examples discussed below the FLM produces results that appear reasonable, but for more accuracy one might employ some special technique, such as singularity removal [*Lowry et al.*, 1989] to improve the approximations.

In our first two test problems below we use the initial condition $h(x, y, z, 0) = 0$ and impose no-flow conditions ($\partial h/\partial z = 0$) on the two horizontal planes representing the impermeable confining layers. In the third problem we impose the condition $h = 0$ at the top of the semipermeable aquitard and a no-flow condition at the bottom of the aquifer. In all three problems we impose the condition $h = 0$ at the vertical planes $x = 0$, $x = X$, $y = 0$, and $y = Y$.

To discretize these problems, we divide the domain $\mathcal{D}$ into J layers that are normal to the z axis. The jth layer has thickness $(\Delta z)_j$, and the aquifer characteristics remain constant within each layer; however, they may vary from layer to layer. Each layer j is bounded above and below by nodal planes $z = z_j$ and $z = z_{j+1}$, so that $(\Delta z)_j = z_{j+1} - z_j$.

At any time t we represent the hydraulic head $h(x, y, z_j, t)$ on a single nodal plane $z = z_j$ by a function $h_j(x, y, t)$ satisfying the prescribed conditions $h_j(0, y, t) = h_j(X, y, t) = h_j(x, 0, t) = h_j(x, Y, t) = 0$ at the vertical boundaries. These conditions allow an exact representation of the (x, y) variations in h_j as a double Fourier sine series, in which the Fourier coefficients Φ_{mnj} are time-dependent:

$$h_j(x, y, t) = \sum_{m=1}^{\infty} \sum_{n=1}^{\infty} \Phi_{mnj}(t) G_{mn}(x, y). \tag{3}$$

Here

$$G_{mn}(x, y) = \sin(n\pi x/X) \sin(m\pi y/Y). \tag{4}$$

For the numerical method we truncate this series, getting an approximation

$$h_j(x, y, t) \approx \sum_{m=1}^{M} \sum_{n=1}^{N} \Phi_{mj}(t) G_{mn}(x, y), \tag{5}$$

where M and N are determined by the level of accuracy desired.

To define the vertical variation of the approximate head $\hat{h}$, we linearly interpolate between nodal planes:

$$\hat{h}(x, y, z, t) = \sum_{j=1}^{J+1} \left[\sum_{m=1}^{M} \sum_{n=1}^{N} \Phi_{mnj}(t) G_{mn}(x, y) \right] N_j(z). \tag{6}$$

Here the functions $N_j(z)$ are standard linear shape functions in the z direction:

$$\begin{aligned} N_j(z) &= 0 && z \geq z_{j+1} \text{ or } z \leq z_{j-1}, \\ N_j(z) &= (z - z_{j-1})/(\Delta z)_{j-1} && z_{j-1} < z \leq z_j, \\ N_j(z) &= (z_{j+1} - z)/(\Delta z)_j && z_j < z \leq z_{j+1}. \end{aligned} \tag{7}$$

To determine the unknown coefficients Φ_{mnj}, we develop a linear system of ordinary differential equations in time by using the following weighted residual equations:

$$\iiint_{\mathcal{D}} \{L[\hat{h}] + F\} w_{m'n'i}\, dx\, dy\, dz = 0. \tag{8}$$

We use as weight functions the shape functions associated with the unknown coefficients Φ_{mnj}, namely,

$$w_{m'n'i}(x, y, z) = N_i(z) G_{m'n'}(x, y). \tag{9}$$

If we interchange the operations of differentiation and integration with the finite summation implicit in $\hat{h}$, (8) becomes

$$\sum_{j=1}^{J+1} \sum_{m=1}^{M} \sum_{n=1}^{N} \iiint_{\mathcal{D}} \{L[\Phi_{mnj} N_j G_{mn}] + F\} \cdot N_i G_{m'n'}\, dx\, dy\, dz = 0. \tag{10}$$

We now integrate by parts to shift one order of differentiation from $\hat{h}$ to the weight function $N_i G_{m'n'}$. In doing so, we simplify matters by observing that the eigenfunctions $G_{mn}(x, y)$ obey orthogonality relationships guaranteeing that, whenever $m \neq m'$ or $n \neq n'$,

$$\int_0^Y \int_0^X G_{mn} G_{m'n'}\, dx\, dy = 0, \tag{11a}$$

$$\int_0^Y \int_0^X \frac{\partial^2 G_{mn}}{\partial x^2} G_{m'n'}\, dx\, dy = 0, \qquad (11b)$$

$$\int_0^Y \int_0^X \frac{\partial^2 G_{mn}}{\partial y^2} G_{m'n'}\, dx\, dy = 0. \qquad (11c)$$

Therefore the only terms that survive the integration and summation in (10) are those for which $m = m'$ and $n = n'$, and we get

$$\sum_{j=1}^{J+1} \Bigg[- \Phi_{mnj} \int_0^Z K_x N_j N_i\, dz \int_0^Y \int_0^X \frac{\partial^2 G_{mn}}{\partial x^2} G_{mn}\, dx\, dy - \Phi_{mnj} \int_0^Z K_y N_j N_i\, dz \int_0^Y \int_0^X \frac{\partial^2 G_{mn}}{\partial y^2} G_{mn}\, dx\, dy - \Phi_{mnj} K_z \frac{\partial N_j}{\partial z} N_i \Big|_0^Z \int_0^Y \int_0^X G_{mn}^2\, dx\, dy + \Phi_{mnj} \int_0^Z K_z \left(\frac{\partial N_j}{\partial z}\right)^2 dz \int_0^Y \int_0^X G_{mn}^2\, dx\, dy + \frac{\partial \Phi_{mnj}}{\partial t} \int_0^Z S_s N_j N_i\, dz \int_0^Y \int_0^X G_{mn}^2\, dx\, dy \Bigg] + Q_{mni} = 0. \qquad (12)$$

Here

$$Q_{mni} = \iiint_{\Omega} F N_i G_{mn}\, dx\, dy\, dz. \qquad (13)$$

One equation of the form (12) holds for each distinct triple (i, m, n) of indices associated with a weight function. For simplicity, we represent the forcing function F by a constant multiple of the Dirac δ distribution $\delta(x, y)$).

As with the usual finite element method using piecewise linear basis functions, terms in (12) for which $|i - j| \geq 2$ vanish, yielding tridiagonal systems with unknowns Φ_{mnj}. If the bottom (or top) of the aquifer is a no-flow boundary, the contributions at $z = 0$ (or $z = Z$) that arise from the integration by parts also vanish. Moreover, owing to the orthogonality relations in (11), each Fourier mode (m, n) has its own matrix equation:

$$[M]_{mn}\Phi_{mn} + [B]_{mn}\, d\Phi_{mn}/dt + \mathbf{Q}_{mn} = \mathbf{0}, \qquad (14)$$

where $[M]_{mn}$ and $[B]_{mn}$ are tridiagonal matrices, and Φ_{mn} and $\mathbf{Q}_{mn}$ are vectors with components Φ_{mnj} and Q_{mnj}, $j = 1, \cdots, N + 1$, respectively. The typical $[M]_{mn}$ and $[B]_{mn}$ tridiagonal entries for a specific layer j (where $1 \leq j \leq J$) are as follows:

$$m_{j1} = \frac{XY}{4}\left\{\left[(K_x)_j\left(\frac{n\pi}{X}\right)^2 + (K_y)_j\left(\frac{m\pi}{Y}\right)^2\right]\frac{(\Delta z)_j}{3} + \frac{(K_z)_j}{(\Delta z)_j}\right\},$$

$$m_{j2} = \frac{XY}{4}\left\{\left[(K_x)_j\left(\frac{n\pi}{X}\right)^2 + (K_y)_j\left(\frac{m\pi}{Y}\right)^2\right]\frac{(\Delta z)_j}{6} - \frac{(K_z)_j}{(\Delta z)_j}\right\},$$

$$m_{j3} = m_{j2},$$

$$m_{j4} = m_{j1},$$

$$b_{j1} = XYS_s(\Delta z)_j/12,$$

$$b_{j2} = b_{j1}/2,$$

$$b_{j3} = b_{j2},$$

$$b_{j4} = b_{j1},$$

Figure 2 depicts how $[M]_{mn}$ and $[B]_{mn}$ are assembled and what entries the 2×2 matrices have.

We approximate the time derivative by a simple difference scheme in Φ:

$$\left.\frac{d\Phi_{mn}}{dt}\right|^{k+\theta} \approx \frac{\Phi_{mn}^{k+1} - \Phi_{mn}^{k}}{\Delta t};$$
$$\Phi_{mn}^{k+\theta} \approx \theta\Phi_{mn}^{k+1} + (1 - \theta)\Phi_{mn}^{k}. \qquad (15)$$

Here k indexes the most recent time level at which Φ_{mn} is known, and $k + 1$ indexes the next time level. We represent the time increment between these two levels by Δt and use θ to denote a weighting parameter, discussed shortly. The temporally discrete system therefore becomes

$$\left\{\theta[M]_{mn} + \frac{1}{\Delta t}[B]_{mn}\right\}\Phi_{mn}^{k+1} = \left\{\frac{1}{\Delta t}[B]_{mn} - (1 - \theta)[M]_{mn}\right\}\Phi_{mn}^{k} - \mathbf{Q}_{mn}^{k}. \qquad (16)$$

Choosing various values of $\theta \in [0, 1]$ yields various temporal weightings of the scheme, with $\theta = 0$ giving an explicit scheme and $\theta = 1$ yielding a fully implicit scheme. We use $\theta = 1/2$, which corresponds to the familiar Crank-Nicolson scheme. This scheme is unconditionally stable and is second-order accurate in t.

3. CODING CONSIDERATIONS

Together with initial conditions and boundary conditions, the model requires the following information: layer-dependent variables, constant within each layer or nodal plane; mode-dependent variables, constant for each Fourier

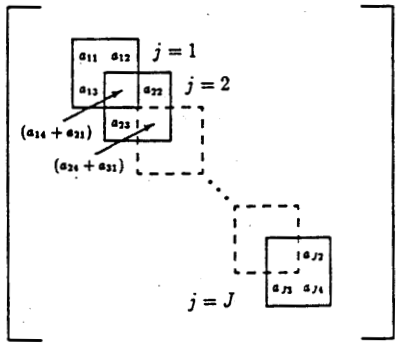

Fig. 2. Matrix assembly for tridiagonal matrices $[M]_{mn}$ and $[B]_{mn}$.

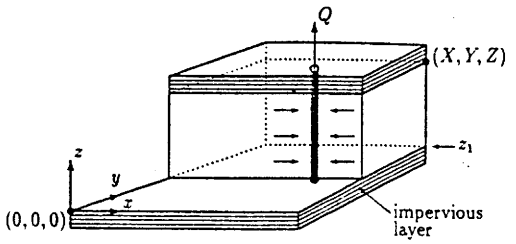

Fig. 3. Geometry of the fully penetrating well.

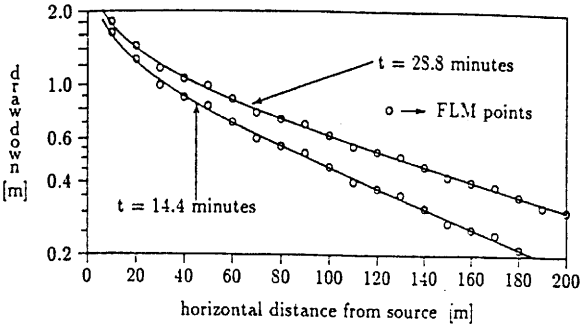

Fig. 4. Hydraulic head h versus distance r from the single, fully penetrating well. Solid curves depict the classical, one-dimensional radial solution.

component; variables characterizing sources (F), and timing variables.

The layer-dependent variables include the number of layers J, the dimensions of each layer, and the conductivities and specific storage of each layer. Variables associated with the Fourier modes include the indices M and N at which the two-dimensional series will be truncated and a matrix [Φ] in which to store Fourier coefficients for each nodal plane. The initial value of [Φ] reflects the initial condition of the aquifer. The variables needed to characterize sources include well locations and volumetric flow rates between nodal planes. The timing variables include the total time t_{total}, the time step Δt, and the temporal weighting parameter θ.

The FLM has advantages in both small-scale and large-scale computing environments. Because the method reduces three-dimensional problems to sets of one-dimensional problems, one can often use a microcomputer to model large, three-dimensional aquifers that would otherwise require too much memory. On the other hand, since the one-dimensional problems are uncoupled, the method is also very adaptable to parallel computing environments. We discuss this possibility further in section 4.

4. Test Problems and Results

We examine four test problems. The first two problems have exact solutions in ideal cases, when the sources have infinitesimal radius and the aquifers have infinite areal extent. The third problem has no exact solution, but there is a classical, closed-form solution that is available if we accept certain simplifying assumptions. The exact solution for the first problem can be used with superposition to obtain an exact solution for the fourth case.

Single, Fully Penetrating Well

Figure 3 depicts a fully penetrating well with a constant discharge rate Q and horizontal flow within the aquifer, and Table 1 summarizes the parameters defining the problem.

TABLE 1. Input Data for the Fully Penetrating Well Problem

	Definition
Depth of aquifer	$Z = 100$ m
Plan dimensions	$X = Y = 1280$ m
Well location	$(x_s, y_s) = (640, 640)$
Hydraulic conductivity	$K = 4$ m/d
Specific storage	$S_s = 1.6 \times 10^{-6}$/m
Discharge rate	$Q = -1257$ m^3/d
Number of modes	$M = N = 32$
Number of layers	$J = 1$
Time step	$\Delta t = 0.001$ day
Total time	$t_{total} = 0.02$ day

The exact solution that we use for comparison is a similarity solution for a line source having infinitesimal radius in a one-dimensional, radial problem, where $r = (x^2 + y^2)^{1/2}$ is the distance from the well. Walton [1970] gives this exact solution as

$$h(r, t) = \frac{Q}{4\pi KZ}\left[-\gamma - \ln u + \sum_{n=1}^{\infty} \frac{(-u)^n}{n(n!)}\right], \quad (17)$$

where $u = (r^2 S_s Z)/(4KZt)$ is the similarity variable and $\gamma \approx 0.5772$ is the Euler constant.

In the numerical model we keep t_{total} small and use large values for X and Y to reduce the influence of the zero-head boundary, since the similarity solution applies to a domain of infinite areal extent. As Figure 4 indicates, the FLM approximation in this case is essentially indistinguishable from the similarity solution.

Point Source Injection

The primary purpose of this test problem is to demonstrate the ability of the layers to model vertical gradients in head. Using a specific storage $S_s = 1.0$ facilitates comparison of the results to the corresponding problem in heat conduction. Figure 5 depicts a point source injection well with a constant injection rate Q, corresponding to a well screened over a small vertical interval. Table 2 summarizes the parameters used to define a sample problem for this geometry. The layer thickness varies from 0.1 to 1.5 m, where we concentrate a large number of layers at and above the point source. The exact solution used for comparison represents radial flow from a point source in a domain having infinite areal extent. *Carslaw and Jaeger* [1959] give this solution as

$$h(r, t) = (Q/4\pi Kr)\ \text{erfc}\ [r/(4Kt)^{1/2}]. \quad (18)$$

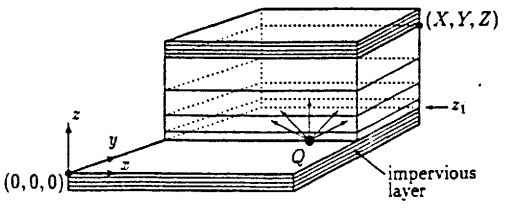

Fig. 5. Geometry of the point source injection well.

TABLE 2. Input Data for the Point Source Injection Well

	Definition
Depth of aquifer	$Z = 32$ m
Plan dimensions	$X = Y = 64$ m
Line source location	$(x_s, y_s) = (32, 32)$
Hydraulic conductivity	$K = 195.3$ m/d
Specific storage	$S_s = 1$ per meter
Injection rate	$Q = 2000$ m^3/d
Number of modes	$M = N = 64$
Number of layers	$J = 50$
Layer thickness	0.1–1.5 m
Time step	$\Delta t = 0.001$ day
Total time	$t_{total} = 0.04$ day

We use a Chebyshev approximation to erfc [see *Press et al.*, 1988]. As in the first sample problem, we keep t_{total} small to avoid the influence of the computational boundaries in the FLM model.

We compare the exact solution with the FLM approximation along two directions from the point source: one on the nodal plane normal to the z axis and one parallel to the z axis. Figures 6 and 7 show these comparisons. As with the fully penetrating well, the FLM gives a good approximation to the exact solution except near the well bore. The discrepancy for $r < 1/2$ m is attributable to the assumption in the exact solution that the source has infinitesimal radius, which implies that the exact solution is unbounded as $r \to 0$. The pressure near the point source remains finite in the FLM solution.

Single Well in a Leaky Aquifer

As a third example we use the FLM to simulate unsteady radial flow in a leaky, isotropic, confined aquifer where a fully penetrating well discharges at a constant rate, as shown in Figure 8. We present two separate runs to illustrate the effectiveness of the FLM model. Table 3 contains the parameters defining them. *Walton* [1970] provides a classical one-dimensional radial solution for this problem, again assuming a well having infinitesimal radius in an aquifer of infinite radial extent:

$$h(r, t) = (Q/4\pi K_A Z_A) W(u, B). \qquad (19)$$

Here K_A and Z_A are the conductivity and depth, respectively, of the aquifer. The well function $W(u, B)$ is represented by the integral

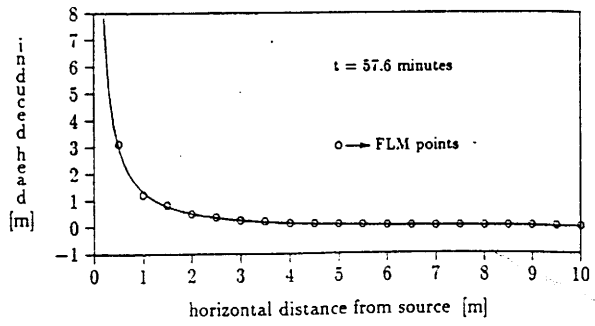

Fig. 6. Numerical and classical solutions for point source injection plotted along the horizontal line $((x, y, z) = (x, y_s, 0))$. The one-dimensional classical solution is depicted by the solid curve.

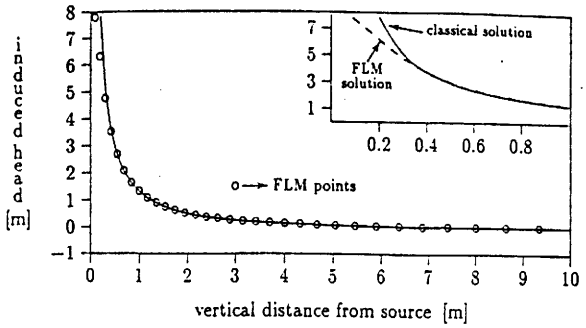

Fig. 7. Numerical and classical solutions for point source injection plotted along the vertical line $((x, y, z) = (x_s, y_s, z))$. The one-dimensional classical solution is depicted by the solid curve. The inset compares the solutions close to the source.

$$W(u, B) = \int_u^\infty \frac{e^{-y}}{y} \exp\left(\frac{-r^2 K_T}{4K_A Z_A Z_T y}\right) dy, \qquad (20)$$

where K_T and Z_T stand for the conductivity and depth of the aquitard. To derive this solution, one must assume that the vertical component of water velocity vanishes in the aquifer. Thus the classical solution unrealistically requires flow lines to be refracted instantaneously from vertical to horizontal as they cross the aquitard-aquifer interface. The classical solution also incorporates the assumption that water is not released from storage in the aquitard. Since $S_s = 0$ in the aquitard, the drawdown varies linearly with elevation, and the vertical velocity is independent of z in the aquitard. As we argue below, the numerical solutions depict more realistic values of the drawdown, capturing a vertical component of velocity in the aquifer and a changing vertical component of velocity in the semipermeable aquitard at early times. As time proceeds, the numerical model approaches the classical solution as expected.

Figure 9 and Figure 10 summarize the first run. Figure 9 shows the drawdown in the classical solution and in the numerical solution generated by the FLM at a radius of 50 m from the source at two time intervals. Figure 10 shows the corresponding values of vertical velocity in the aquitard. The vertical velocity in the aquifer is essentially constant at about 0.001 m/d. The FLM solution at $t = 2.88$ min illustrates the effects of storage in the semipermeable layer, which the classical model cannot capture. Figure 11 depicts the results of the second run in a log-log format, at an elevation of 15 m. These results are representative of those obtainable from the classical solution. However, the FLM method allows one to distinguish well function values asso-

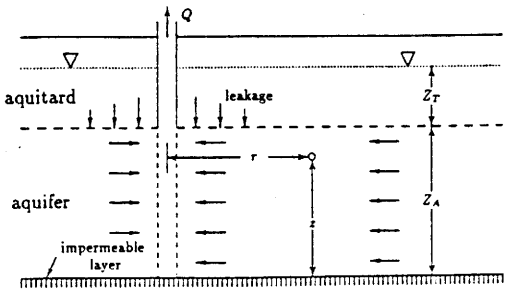

Fig. 8. Geometry of a single well in a leaky aquifer.

TABLE 3. Input Data for the Single Well in a Leaky Aquifer

	Definition
Total depth	$Z = Z_A + Z_T = 80$ m
Aquifer depth	$Z_A = 60$ m
Aquitard depth	$Z_T = 20$ m
Plan dimensions	
Run 1	$X = Y = 1280$ m
Run 2	$X = Y = 3200$ m
Well location	
Run 1	$(x_s, y_s) = (640, 640)$
Run 2	$(x_s, y_s) = (1600, 1600)$
Aquifer conductivity	$K_A = 25$ m/d
Aquitard conductivity	$K_T = 0.12$ m/d
Aquifer specific storage	$S_{sA} = 2.0 \times 10^{-6}$/m
Aquitard specific storage	$S_{sT} = 1.5 \times 10^{-6}$/m
Discharge rate	$Q = 18.850$ m^3/d
Number of modes	$M = N = 64$
Number of layers	$J = 120$
Layer thickness	0.1–15 m
Time step	$\Delta t = 0.0001$–0.001 day

ciated with different elevations within the aquifer, which the classical solution does not. The inset in Figure 11 shows the well function values at different elevations, 15 and 59 m.

Multiwell Field

The primary purpose of the fourth test case is to demonstrate the ability of the FLM to model a multiwell field. Our example has three fully penetrating wells. The first well discharges at a constant rate starting at $t = 0$. The second and third wells inject at constant rates starting at $t = 0.002$ day. Table 4 summarizes the parameters defining the problem. The exact solution that we use for comparison is a superposition of similarity solutions like those used for the first problem.

In the numerical model we keep t_{total} small and use large values for X and Y to reduce the influence of the zero-head boundary, since the similarity solution applies to a domain of infinite areal extent. We compare numerical and exact solutions along the transect $y = 600$ m, which passes close to the three wells. As Figure 12 indicates, the FLM approximation for the case $M = N = 32$ shows virtually no spurious oscillations, being essentially indistinguishable from the similarity solution. At the coarser level of Fourier discretization in which $M = N = 16$, the numerical solution is still reasonable, but some overshooting and oscillations, attributable to the Gibbs phenomenon, are apparent.

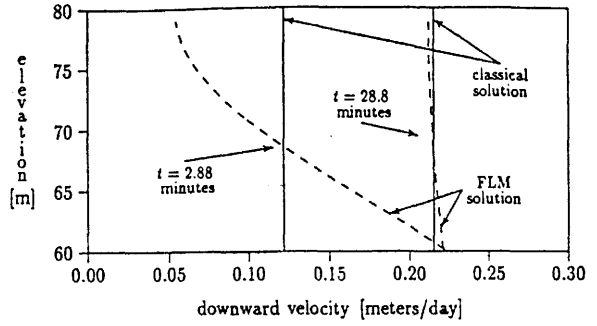

Fig. 10. Vertical velocity in aquitard for the leaky aquifer problem at 50 m from the well, shown at two different times. The solid curve depicts the one-dimensional radial solution, and the dashed curves depict the FLM solution.

Parallelization

Although one can run all of our test problems on a personal computer by sequentially solving the tridiagonal matrix equations for the Fourier modes, it is noteworthy that our code is also amenable to parallel processing. To demonstrate this fact, we present results of the second test problem run on an Alliant FX/8 computer having a shared memory and eight vector processors. Parallelization in a FLM model consists of sending distinct tridiagonal systems to different processors, which then execute the solution algorithm concurrently until all Fourier modes have been computed.

To quantify the efficiency of the parallelization, we examine the CPU time required to solve problems using different numbers p of processors. For each value of p the speedup S_p is the ratio of the time taken by one processor in solving the problem to the time required for p processors. For an ideally parallel algorithm a plot of S_p versus p, called a speedup curve, yields a line having unit slope. In practice, the need for processors to transfer information among themselves prohibits this ideal case, and speedup curves having average slope greater than 0.7 typically indicate excellent parallelism. Figure 13 shows the speedup curve for the second test problem, where $M = N = 64$. The ideal curve is represented by the top curve and has unit slope. The CPU time ratio which was required for just the FLM parallel algorithms is depicted by the lower curve and has a slope of approximately 0.8. For much larger values of M and N we expect the speedups to be somewhat less favorable on shared-memory machines because of computational overhead asso-

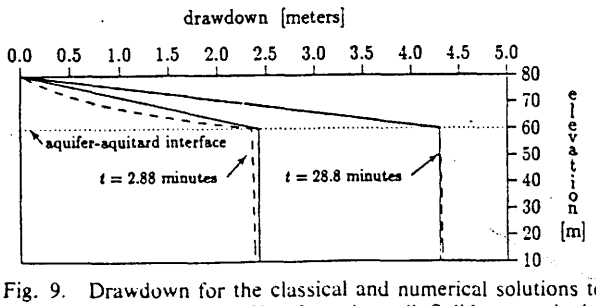

Fig. 9. Drawdown for the classical and numerical solutions to the leaky aquifer problem at 50 m from the well. Solid curves depict the one-dimensional radial solution, and the dashed curves depict the FLM solution.

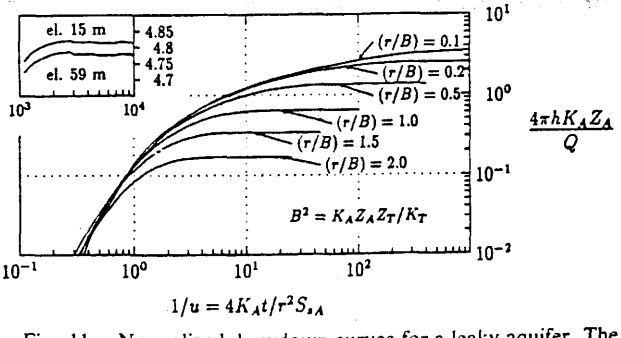

Fig. 11. Normalized drawdown curves for a leaky aquifer. The inset shows the drawdowns at two different depths, as predicted by the FLM model.

TABLE 4. Input Data for the Multiwell Problem

	Definition
Depth of acquifer	$Z = 100$ m
Plan dimensions	$X = Y = 1280$ m
Location	
Well 1	$(x_s, y_s) = (640, 640)$
Well 2	$(x_s, y_s) = (480, 560)$
Well 3	$(x_s, y_s) = (640, 440)$
Hydraulic conductivity	$K = 4$ m/d
Specific storage	$S_s = 1.6 \times 10^{-6}$/m
Discharge rate	
Well 1	$Q = -1257$ m^3/d
Injection rate	
Well 2	$Q = +1000$ m^3/d
Well 3	$Q = +257$ m^3/d
Number of modes	
Run 1	$M = N = 16$
Run 2	$M = N = 32$
Start time	
Well 1	$t = 0.0$
Well 2	$t = 0.002$ day
Well 3	$t = 0.002$ day
Number of layers	$J = 1$
Time step	$\Delta t = 0.001$ day
Total time	$t_{total} = 0.02$ day

ciated with the retrieval of data from cache. For such large-scale problems it is likely that distributed memory machines offer a more effective parallel environment.

5. CONCLUSIONS

The FLM offers a numerical approach for modeling aquifer problems having reasonably regular, layered geometry. The method's attractiveness stems from its ability to capture three-dimensional aspects of aquifer behavior in a highly parallelizable fashion, without the intensive computational requirements associated with fully three-dimensional matrices arising in traditional finite element methods. Of course, for complicated heterogeneities the simplified geometry assumed by the FLM is inadequate, and fully three-dimensional models are needed.

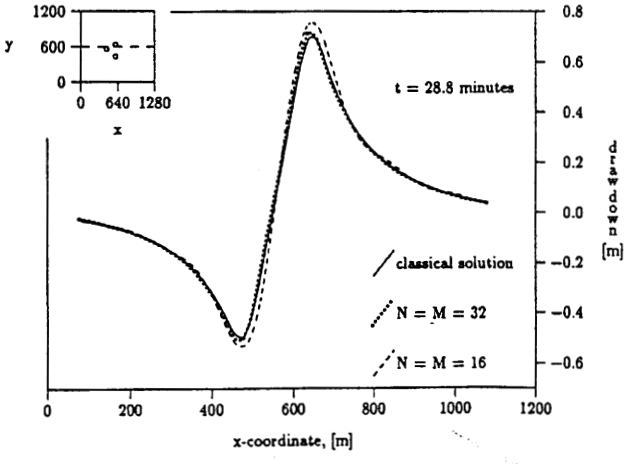

Fig. 12. Drawdown along the transect $(x, y, z) = (x, 600, z)$ for the multiwell problem. Shown are the exact solution and numerical solutions for two different Fourier discretizations. The inset shows the location of the transect (dashed line) with respect to the three wells.

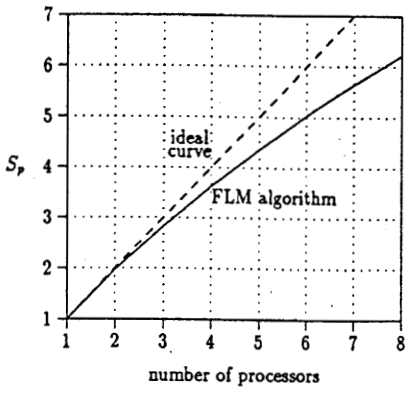

Fig. 13. Speedup curve for FLM model on Alliant FX/8 parallel computer.

We see tremendous potential for the FLM in developing rapidly executable models of groundwater flow. The method's inherent parallelism may make it an attractive choice for applications that require repeated execution, since iteratively running such standard flow codes as MODFLOW [*McDonald and Harbaugh*, 1984] can be prohibitively slow. This advantage can be especially important, for example, in optimization studies and inverse problems.

NOTATION

Dimensions appear in square brackets.

$[B]_{mn}$ finite element stiffness matrix for Fourier mode mn.
$\mathfrak{D}$ three-dimensional domain, $(0, X) \times (0, Y) \times (0, Z)$.
F forcing function $[1/T]$.
$G_{mn}(x, y)$ double sine or cosine function.
h hydraulic head $[L]$.
$\hat{h}$ trial function for hydraulic head $[L]$.
h_j hydraulic head on nodal plane j $[L]$.
i, j nodal plane subscripts; $1 \le i, j \le J + 1$.
J number of layers.
$k, k + 1$ time level superscripts, old and new, respectively.
K_x hydraulic conductivity in the x direction $[L/T]$.
$L[\ ]$ differential operator for transient groundwater flow.
$[M]_{mn}$ finite element mass matrix for a specific Fourier mode, mn.
m, n Fourier mode subscripts.
M, N truncation levels for Fourier series; $1 \le m \le M$ and $1 \le n \le N$.
$N_j(z)$ linear shape function.
p number of processors.
$\mathbf{Q}_{mn}$ forcing vector, equal to $(Q_{mn1}, Q_{mn2}, \cdots, Q_{mn(N+1)})^T$.
Q_{mnj} variational form of forcing function.
r radial distance from line and point sources $[L]$.
S_p speedup.
S_s specific storage $[L^{-1}]$.
t time $[T]$.
t_{total} total time of simulation $[T]$.

u	similarity variable.
$W(u, B)$	well function.
x, y, z	spatial coordinates (z is elevation above datum) [L].
X, Y, Z	dimensions of finite spatial domain [L].
x_s, y_s, z_s	coordinate of point source or line source [L].
z_i	elevation of layer i; $1 \le i \le J + 1$ [L].
Δt	time step [T].
$(\Delta z)_i$	thickness of layer [L].
$[\Phi]$	matrix composed of vectors Φ_{mn}.
Φ_{mn}	vector of Fourier coefficients, equal to $(\Phi_{mn1}, \Phi_{mn2}, \cdots, \Phi_{mn(N+1)})^T$.
$\Phi_{mnj}(t)$	Fourier coefficient for nodal plane j.
θ	temporal weighting parameter; $0 \le \theta \le 1$.

Acknowledgments. The Wyoming Water Research Center supported this work through a grant in aid. We also received support from NSF grant RII-8610680 and ONR grant 0014-88-K-0370.

REFERENCES

Booker, J. R., and J. C. Small, Finite layer analysis of consolidation, I, *Int. J. Numer. Anal. Methods Geomech.*, *6*(2), 151–171, 1982*a*.

Booker, J. R., and J. C. Small, Finite layer analysis of consolidation, II, *Int. J. Numer. Anal. Methods Geomech.*, *6*(2), 173–194, 1982*b*.

Booker, J. R., and J. C. Small, Finite layer analysis of viscoelastic layered materials, *Int. J. Numer. Anal. Methods Geomech.*, *10*(4), 415–430, 1986.

Carslaw, H. S., and J. C. Jaeger, *Conduction of Heat in Solids*, 2nd ed., Oxford University Press, New York, 1959.

Cheung, Y.-K., *Finite Strip Method in Structural Mechanics*, Pergamon, New York, 1976.

Cheung, Y.-K., and S. C. Fan, Analysis of pavements and layered foundations by finite layer method, in *Proceedings of the Third International Conference on Numerical Methods in Geomechanics*, pp. 1129–1135, edited by W. Wittke, A. A. Balkema, Rotterdam, Netherlands, 1979.

Gottlieb, D., and S. A. Orszag, *Numerical Analysis of Spectral Methods: Theory and Applications*, Society for Industrial and Applied Mathematics, Philadelphia, Pa., 1977.

Huyakorn, P. S., and G. F. Pinder, *Computational Methods in Subsurface Flow*, Academic, San Diego, Calif., 1983.

Hwang, J. S., C. J. Chen, M. Sheikhoslami, and B. K. Panigrahi, Finite analytic solution for two-dimensional groundwater solute transport, *Water Resour. Res.*, *21*(9), 1354–1360, 1985.

Lowry, T., M. B. Allen, and P. N. Shive, Singularity removal: A refinement of resistivity modeling techniques, *Geophysics*, *54*(6), 766–774, 1989.

McDonald, M. G., and A. W. Harbaugh, A modular three-dimensional finite-difference ground-water flow model, *U.S. Geol. Surv. Open File Rep.*, *83-875*, 1984.

Press, W. H., B. P. Flannery, S. A. Teukolsky, and W. T. Vetterling, *Numerical Recipes in C, The Art of Scientific Computing*, Cambridge University Press, New York, 1988.

Puckett, J. A., and R. J. Schmidt, Finite strip method for groundwater modeling in a parallel computing environment, *Eng. Comp.*, *7*(2), 1990.

Puckett, J. A., and D. L. Wiseman, Recent developments in the finite strip methods, paper presented at the Structures Congress, Am. Soc. Civ. Eng., Orlando, Fla., Aug. 1987.

Rowe, R. K., and J. R. Booker, Finite layer analysis of nonhomogeneous soils, *J. Eng. Mech. Div., Am. Soc. Civ. Eng.*, *108*(EM1), 115–132, 1982.

Slattery, J. E., *The Finite Strip Method in Groundwater Hydrology*, M.S. thesis, Colorado State Univ., Fort Collins, 1986.

Small, J. C., and J. R. Booker, Finite layer analysis of layered elastic materials using a flexibility approach, 1, Strip loadings, *Int. J. Numer. Methods Eng.*, *20*(6), 1025–1037, 1984*a*.

Small, J. C., and J. R. Booker, Surface deformation of layered soil deposits due to extraction of water, in *Ninth Australasian Conference on the Mechanics of Structures and Materials*, vol. 9, pp. 33–38, University of Sydney, School of Civil and Mining Engineering, Sydney, Australia, 1984*b*.

Sudicky, E. A., The Laplace transform Galerkin technique: A time-continuous finite element theory and application to mass transport in groundwater, *Water Resour. Res.*, *25*(8), 1833–1846, 1989.

Walton, W. C., *Groundwater Resource Evaluation*, McGraw-Hill, New York, 1970.

M. B. Allen and S. S. Smith, Department of Mathematics, University of Wyoming, Box 3036, Laramie, WY 82071.

T. Edgar and J. Puckett, Department of Civil Engineering, University of Wyoming, Box 3295, Laramie, WY 82071.

(Received April 1, 1991;
revised February 5, 1992;
accepted February 13, 1992.)